

**U-Load  
Dextramer®**

Build multimers with your choice of peptide and peptide-receptive MHC I and MHC II alleles.



This information is current as of February 26, 2022.

## **Radiosensitive Hematopoietic Cells Determine the Extent of Skin Inflammation in Experimental Epidermolysis Bullosa Acquisita**

Hiroaki Iwata, Mareike Witte, Unni Krishna S. R. L. Samavedam, Yask Gupta, Atsushi Shimizu, Akira Ishiko, Tobias Schröder, Karsten Seeger, Markus Dahlke, Dirk Rades, Detlef Zillikens and Ralf J. Ludwig

*J Immunol* 2015; 195:1945-1954; Prepublished online 22 July 2015;  
doi: 10.4049/jimmunol.1501003  
<http://www.jimmunol.org/content/195/5/1945>

**Supplementary Material** <http://www.jimmunol.org/content/suppl/2015/07/22/jimmunol.1501003.DCSupplemental>

**References** This article **cites 39 articles**, 11 of which you can access for free at:  
<http://www.jimmunol.org/content/195/5/1945.full#ref-list-1>

**Why *The JI*? Submit online.**

- **Rapid Reviews! 30 days\*** from submission to initial decision
- **No Triage!** Every submission reviewed by practicing scientists
- **Fast Publication!** 4 weeks from acceptance to publication

*\*average*

**Subscription** Information about subscribing to *The Journal of Immunology* is online at:  
<http://jimmunol.org/subscription>

**Permissions** Submit copyright permission requests at:  
<http://www.aai.org/About/Publications/JI/copyright.html>

**Email Alerts** Receive free email-alerts when new articles cite this article. Sign up at:  
<http://jimmunol.org/alerts>



# Radiosensitive Hematopoietic Cells Determine the Extent of Skin Inflammation in Experimental Epidermolysis Bullosa Acquisita

Hiroaki Iwata,<sup>\*,1</sup> Mareike Witte,<sup>†</sup> Unni Krishna S. R. L. Samavedam,<sup>†</sup> Yask Gupta,<sup>†</sup> Atsushi Shimizu,<sup>‡</sup> Akira Ishiko,<sup>‡</sup> Tobias Schröder,<sup>†</sup> Karsten Seeger,<sup>§</sup> Markus Dahlke,<sup>¶</sup> Dirk Rades,<sup>¶</sup> Detlef Zillikens,<sup>\*,†</sup> and Ralf J. Ludwig<sup>\*,†</sup>

Animal models have enhanced our understanding of the pathogenesis of autoimmune diseases. For these models, genetically identical, inbred mice have commonly been used. Different inbred mouse strains, however, show a high variability in disease manifestation. Identifying the factors that influence this disease variability could provide unrecognized insights into pathogenesis. We established a novel Ab transfer-induced model of epidermolysis bullosa acquisita (EBA), an autoimmune disease characterized by (muco)-cutaneous blistering caused by anti-type VII collagen (COL7) autoantibodies. Blistering after anti-COL7 IgG (directed against the von Willebrand factor A-like domain 2) transfer showed clear variability among inbred mouse strains, that is, severe cutaneous blistering and inflammation in C57BL/6J and absence of skin lesions in MRL/MpJ mice. The transfer of anti-COL7 IgG into irradiated, EBA-resistant MRL/MpJ mice, rescued by transplantation with bone marrow from EBA-susceptible B6.AK-H2k mice, induced blistering. To the contrary, irradiated EBA-susceptible B6.AK-H2k mice that were rescued using MRL/MpJ bone marrow were devoid of blistering. In vitro, immune complex activation of neutrophils from C57BL/6J or MRL/MpJ mice showed an impaired reactive oxygen species release from the latter, whereas no differences were observed after PMA activation. This finding was paralleled by divergent expression profiles of immune complex-activated neutrophils from either C57BL/6J or MRL/MpJ mice. Collectively, we demonstrate that radiosensitive cells determine the varying extent of skin inflammation and blistering in the end-stage effector phase of EBA. *The Journal of Immunology*, 2015, 195: 1945–1954.

**A**utoimmune diseases, such as systemic lupus erythematosus, rheumatoid arthritis, type 1 diabetes, or autoimmune bullous dermatoses, are examples of complex diseases that have become a major health burden worldwide (1). They are characterized by an aberrant immune response against self-Ags (2), which is, for example, reflected by the detection of autoantibodies in patients (3) and the demonstration of autoantibody pathogenicity by transfer into experimental animals (4). Although the current treatment options for patients with autoim-

mune diseases are far from ideal, they have dramatically improved, as exemplified by the introduction and application of biologicals into clinical practice (5). The present treatment of patients with autoimmune diseases has been shaped, to a great extent, by an increased understanding of the pathogenesis of diseases. In particular, the development and use of animal models have significantly contributed to both an increased understanding of the pathogenesis of autoimmune diseases and the identification of novel treatments (6).

For several reasons, such as the reproduction rate, housing requirements, standardization, and availability of genetic modifications, inbred mice are most often used in current biomedical research. Translating the experimental outcomes from mouse models into the corresponding human diseases may, however, be hampered by conflicting and contradictory results obtained from different inbred mouse lines, that is, a reduced response to i.v. Ig treatment of immune thrombocytopenia in C57BL/6, as opposed to BALB/c, mice (7). Consistent with this observation of a differential response to treatment, disease induction in mice is strain dependent. This strain dependency has been identified for both immunization-induced (8, 9) and Ab transfer-induced models of autoimmune diseases (10, 11). These observations led to the identification of the C5 locus as an important modulator of joint destruction in the K/B×N serum transfer arthritis model (10). Therefore, novel insights into the pathogenesis of disease and therapeutic responses can be obtained from a detailed understanding of strain differences observed in the majority, if not all, of mouse models of autoimmune diseases.

In this study, we developed a novel Ab transfer-induced mouse model of epidermolysis bullosa acquisita (EBA), which is a rare but prototypical organ-specific autoimmune disease caused by autoantibodies against type VII collagen (COL7) (12, 13). Al-

\*Department of Dermatology, University of Lübeck, D-23538 Lübeck, Germany;

<sup>†</sup>Lübeck Institute of Experimental Dermatology, University of Lübeck, D-23538 Lübeck, Germany; <sup>‡</sup>First Department of Dermatology, School of Medicine, Faculty of Medicine Toho University, Tokyo 143-8540, Japan; <sup>§</sup>Department of Chemistry, University of Lübeck, D-23538 Lübeck, Germany; and <sup>¶</sup>Department of Radiation Oncology, University of Lübeck, D-23538 Lübeck, Germany

<sup>1</sup>Current address: Department of Dermatology, Hokkaido University Graduate School of Medicine, Sapporo, Japan.

Received for publication April 30, 2015. Accepted for publication June 26, 2015.

This work was supported in part by Deutsche Forschungsgemeinschaft Grants DFG LU877/10-1, GRK 1727/1 (Research Training Group "Modulation of Autoimmunity"), GRK 1743/1 (Research Training Group "Genes, Environment, and Inflammation"), and EXC 306/2 (Excellence Cluster "Inflammation at Interfaces").

The expression data presented in this article have been submitted to Gene Expression Omnibus under accession number GSE70193.

Address correspondence and reprint requests to Prof. Ralf J. Ludwig, Lübeck Institute of Experimental Dermatology, University of Lübeck, Ratzeburger Allee 160, D-23538 Lübeck, Germany. E-mail address: ralf.ludwig@uksh.de

The online version of this article contains supplemental material.

Abbreviations used in this article: COL7, type VII collagen; DEJ, dermal-epidermal junction; EBA, epidermolysis bullosa acquisita; IC, immune complex; IF, immunofluorescent; ROS, reactive oxygen species; vWFA2, von Willebrand factor A-like domain 2.

Copyright © 2015 by The American Association of Immunologists, Inc. 0022-1767/15/\$25.00

though the clinical presentation of EBA patients shows considerable variability, that is, EBA patients may present with skin fragility, tense blisters, scarring, milia formation, or widespread cutaneous blistering on inflamed skin, which is often complicated by mucous membrane involvement (14–16), subepidermal blistering is the histopathological hallmark of the disease (17).

In the current study, we first demonstrated the *in vitro* and *in vivo* pathogenicity of autoantibodies directed against an immunodominant epitope located within the murine COL7. Secondly, our results confirmed observations of strain dependency in Ab transfer model of arthritis (10) and nephritis (11). By generating bone marrow chimeric mice, we extended these findings, thus demonstrating that the observed strain dependency in Ab transfer-induced EBA is uniquely controlled by radiosensitive cells. Because Gr-1<sup>+</sup> myeloid cells are the primary effector cells in Ab transfer-induced EBA (6), we subsequently investigated the transcriptional and functional responses of neutrophils from EBA-resistant and EBA-susceptible mouse strains. Pathway analysis of this data set provided novel insights into the molecular mechanisms of neutrophil activation.

## Materials and Methods

### Studies involving human material

The approval for studies using biological material from humans was obtained from the Institutional Review Board at the University of Lübeck (Lübeck, Germany), and written informed consent was obtained, as specified in the Declaration of Helsinki.

### Mice

Mice from inbred mouse strains (BALB/cJ, C57BL/6J, DBA/1J, and MRL/MpJ); B6.129P2-Fcγr1gtn1Rav/J (γ-chain deficient), B10.D2-Hc0 H2d H2-T18c/oSnJ (C5-deficient), and B10.D2-Hc1 H2d H2-T18c/nSnJ (C5-sufficient); and MHC-congenic B6.C-H2d/bByJ (B6.d), B6.SJL-H2s C3c/IcYJ (B6.s), and B6.AK-H2k/FlaEgJ (B6.k) were obtained from The Jackson Laboratory (Bar Harbor, ME). Sixth generation mice of a recently described, autoimmune-prone advanced intercross line were made, as previously described (18). All animals were housed in specific pathogen-free conditions, fed standard mouse chow, and provided acidified drinking water *ad libitum*. All clinical examinations, biopsies, and blood drawings were performed under anesthesia using *i.p.* administration of a mixture of ketamine (100 μg/g) and xylazine (15 μg/g). The animal experiments were approved by the local authorities of the Animal Care and Use Committee (Kiel, Germany) and conducted by certified personnel.

### Generation of bone marrow chimeric mice

Bone marrow from B6.k or MRL/MpJ mouse donors was isolated from femoral bones. The cells ( $1 \times 10^7$ ;  $6.7 \times 10^6$ /ml) were *i.v.* injected into irradiated (8 Gy) B6.k and MRL/MpJ female mice. Engraftment of donor cells was evaluated using flow cytometry 6 wk after transplantation. EDTA-anticoagulated blood was stained with PE-CD8a (clone 53-6.7; eBioscience, Frankfurt, Germany) and FITC-CD8b.2 (clone 53-5.8; BioLegend, San Diego, CA) to distinguish the different alloantigens of the MRL/MpJ and B6.k strains (19, 20).

### Induction of experimental EBA and clinical evaluation

Experimental EBA was induced by repetitive injections of anti-COL7<sup>vWFA2</sup> IgG, according to slightly modified established protocols (21). Two New Zealand White rabbits (SA6812 and SA6813) were *s.c.* immunized with 250 μg murine von Willebrand factor A-like domain 2 (vWFA2) protein (13, 22) that was suspended in CFA. The animals were boosted three times (at 13-d intervals) with the same protein preparation in IFA, and immune sera were characterized using immunofluorescent (IF) microscopy on cryosections of murine skin. IgG from immune and normal rabbit sera was purified using affinity chromatography and protein G affinity, as previously reported (23, 24). The split-inducing capacity of the purified rabbit Abs was evaluated using an *in vitro* assay, as described elsewhere (25–27). The reactive oxygen species (ROS) release capacity of the purified rabbit Abs was studied using an established *in vitro* assay (28). In cases of ROS release by mouse neutrophils, the cells were isolated from bone marrow flushed from femurs and tibias, as previously reported (29). In brief, neutrophils were isolated from cell suspension using 62% Percoll (GE

Healthcare, Uppsala, Sweden). After centrifugation at  $1000 \times g$  for 30 min at room temperature without breaking, the pellet was collected. The cells were subsequently washed with RPMI 1640 medium (Lonza, Basel, Switzerland) and resuspended at  $2 \times 10^7$  cells/ml in phenol red-free RPMI 1640 medium (Biochrom, Berlin, Germany) supplemented with 25 mM HEPES and 1% FCS. PMA (2 μg/ml) was then used as a positive control. Purified rabbit IgG specific to vWFA2 or normal rabbit IgG was injected *s.c.* into adult mice every second day for a total of six injections. The mice were examined to determine their general condition and to note evidence of cutaneous lesions (*i.e.*, erythema, blisters, erosions, alopecia, and crusts) every fourth day for 12 or 20 d. Disease severity is expressed as the percentage of body surface area that was affected by skin lesions every fourth day, and total disease severity during the observation period was calculated as the area under the curve of the recorded disease severity. Serum and tail skin samples were collected every fourth day. Serum, ear skin, tail skin, oral mucosa, esophagus, stomach, duodenum, small intestine, and colon samples were obtained on the final day and prepared for examination by histopathology and IF microscopy. Skin samples for electron microscopy were obtained on days 6 and 20.

### Direct and indirect IF microscopy, immunoblot analysis, and histopathology

Tissue-bound Abs were detected using direct IF microscopy on 6-μm frozen sections that were prepared from tissue biopsies using 100-fold diluted FITC-labeled Abs specific to rabbit IgG (DakoCytomation) or murine C3 (Cappel Organon-Teknika). The fluorescence intensity at the dermal-epidermal junction (DEJ) was determined using ImageJ software (<http://rsbweb.nih.gov/ij/>) and dermal fluorescence for background subtraction. NaCl (1 M)-split murine and human skin sections were prepared, as previously described (30). Recombinant vWFA2 proteins or murine dermal extracts were fractionated using 12 and 6% SDS-PAGE, respectively, transferred to nitrocellulose, and analyzed using immunoblotting (31). The dermal extracts were prepared as described (32). H&E staining and direct and indirect IF microscopy were performed as described (33).

### Expression profiling of immune complex-activated mouse neutrophils

Gene expression in immune complex (IC)-activated neutrophils of MRL/MpJ and C57BL/6J mice and nonactivated neutrophils from gender-, age-, and strain-matched mice was compared using the Affymetrix GeneChip Mouse Gene 2.0 ST Array ( $n = 3$ /group). The raw data were processed using the oligo R/BioConductor package. Thus, the raw intensity values were background corrected, log<sub>2</sub> transformed, and then quantile normalized using the Robust Multichip Average implemented in R. An unpaired *t* test was performed to identify differentially expressed genes. Genes with a fold change of  $>2$  or  $\leq 2$  and  $p < 0.01$  were considered to be statistically significant. The pathway ontology was performed using the Database for Annotation, Visualization, and Integrated Discovery v6.7 as well as the STRING database with Kyoto Encyclopedia of Genes and Genomes as a reference pathway database. Moreover, ingenuity pathway analysis software was used to investigate the unknown putative pathways. For the generation of heat maps, we used the gplots package provided by R.

### Statistical analysis

Comparisons or differences in the extent of clinical phenotypes were performed using SigmaPlot (Version 12; Systat Software, Erkrath, Germany). The tests used are presented in the legends of the figures and tables. A *p* value  $<0.05$  was considered to be statistically significant.

## Results

### Mice injected with Abs against the vWFA2-like domain of murine COL7 develop skin blisters

*In vitro* characterization of anti-COL7 (vWFA2) IgG. IgG from immune rabbit sera (SA6812 and SA6813) against the COL7 subdomain vWFA2, but not preimmune sera, bound to the DEJ of murine skin as determined by indirect IF microscopy (Supplemental Fig. 1A, 1B). Immune IgG localized at the dermal side of 1 M NaCl-split murine skin (Supplemental Fig. 1C) with an endpoint serum titer by indirect IF of 1:256,000. Cross-reactivity at lower endpoint titers (1:800) with human skin was also observed (Supplemental Fig. 1D). Indirect immunogold electron microscopy with murine skin as a substrate showed immune IgG deposits at the lamina densa (Supplemental Fig. 1E).



Using immunoblot analysis, immune sera, but not preimmune sera, targeted both recombinant vWFA2 protein and dermal extract of murine skin at 290 kDa (Supplemental Fig. 1F, 1G). To study the pathogenic potential of immune IgG, we first evaluated the impact of immune IgG/vWFA2 IC on neutrophil activation. Incubation of neutrophils with either Ag or immune IgG alone did not lead to their activation assayed by their ROS release. In contrast, incubation of neutrophils with IC dose dependently activated neutrophils, exceeding the ROS release of the positive control (fMLP) (Supplemental Fig. 1H). To study the ability to induce subepidermal splits *ex vivo*, immune IgG was incubated with cryosections of murine skin. After the subsequent addition of leukocytes, subepidermal splits developed in skin sections incubated with immune IgG (Supplemental Fig. 1I, 1J), whereas no dermal–epidermal separation occurred in sections treated with preimmune IgG (Supplemental Fig. 1K).

**Anti-COL7 (vWFA2) IgG dose dependently induces subepidermal blisters in mice.** To clarify whether anti-COL7 (vWFA2) IgG is capable of inducing skin blistering *in vivo*, C57BL/6J male mice were injected with immune IgG. Injecting 0.25 mg/g immune IgG led to the induction of subepidermal blisters in C57BL/6J mice ( $n = 16$ ). Disease severity, determined as the body surface area affected by skin lesions, increased throughout the observation period (Fig. 1A). To confirm these results in an independent experiment and to establish a possible dose–response relationship, mice received 0.25, 0.125, or 0.063 mg/g immune IgG per injection. Again, subepidermal blistering was observed in all mice. The onset of disease and the extent of blistering were, however, dose dependent. The mice injected with high and medium immune IgG doses developed skin lesions within 4 d after the first injection, whereas the mice injected with 0.063 mg/g developed initial skin lesions by day 8 and had an overall reduced cumulative disease severity, expressed as the area under the curve calculated from the plots of affected body surface area against time (Fig. 1B, 1C). In all of the mice injected with immune IgG, skin lesions initially developed on the ears and eyelids. Subsequently, the lesions spread to tails, limbs, and trunk. Most commonly, erosions, crusts, and alopecia were observed (Fig. 1D, 1F). In all mice injected with immune IgG, light-microscopic analysis of skin biopsies revealed extensive subepidermal blisters accompanied by varying degrees of inflammatory infiltrates (Fig. 1G). Transmission electron microscopy showed that blisters developed below the lamina densa (Fig. 1H). Furthermore, deposits of IgG and C3 were observed at the DEJ of mice injected with immune IgG (Fig. 1I, 1J), and the degree of IgG deposits at the DEJ increased over time (Fig. 1K). Regarding other anatomical sites, 7 (46.8%) of 15 oral mucosa and 5 (33.3%) of 15 esophagus specimens showed subepidermal blistering with mild inflammatory infiltrates (Supplemental Fig. 2A). Additionally, failure to gain weight was observed in the diseased mice, but not in the control mice. Control mice gained 13% weight during the 20-d observation period. In contrast, the diseased mice only gained 1% weight (Supplemental Fig. 2B).

**Anti-COL7 (vWFA2) IgG-induced blistering depends on activating  $Fc\gamma R$ s and C5.** The  $\gamma$ -chain (Fcer1)–deficient mice were completely resistant to induction of experimental EBA; moreover, doses of 0.5 mg/g immune IgG did not lead to the development of skin lesions (Supplemental Fig. 3). Histopathologically, neither subepidermal blistering nor leukocyte infiltration was observed (data not shown). Direct IF microscopy showed linear deposits of rabbit IgG and murine C3 in all  $\gamma$ -chain–deficient mice injected with immune IgG (Supplemental Fig. 3). In contrast, the control mice in this experiment developed clinical disease (Supplemental Fig. 3). Interestingly, both C5-deficient and C5-sufficient mice ( $n = 12/10$ ) developed initial blisters 4–6 d after the first injection of immune

IgG (Supplemental Fig. 3). C5-deficient mice, however, presented with a significantly milder blistering phenotype compared with C5-sufficient mice. Reductions by 76, 78, or 88% were observed in mice injected with 0.125, 0.25, and 0.5 mg/g immune IgG, respectively. Histopathologically, subepidermal blistering was observed in biopsies of lesional skin in both groups (data not shown). Direct IF microscopy of skin showed linear deposits of rabbit IgG and murine C3 (Supplemental Fig. 3), with similar intensities in both groups.

#### *Induction of skin blistering is strain dependent*

In Ab-transfer mouse models of arthritis and nephritis, a high variability of disease severity among different inbred strains has been observed (10, 11). Previous data in Ab transfer-induced EBA also pointed toward a strain dependency of autoantibody-induced blistering because C57BL/6 mice presented with nearly a 2-fold increase in body surface area affected by subepidermal blistering compared with BALB/c mice (34). To systematically analyze for a potential strain dependency of Ab transfer-induced EBA, C57BL/6J, DBA/1J, BALB/c, and MRL/MpJ ( $n = 4$ ) mice were concurrently injected with 0.125 mg/g anti-COL7 (vWFA2) IgG, which duplicates the immunological, histological, and clinical features of the inflammatory variant of the human disease, as well as of other Ab transfer-induced EBA mouse models (Fig. 1). C57BL/6J and BALB/c mice, but not MRL mice, developed clinical disease, which was most pronounced in C57BL/6J mice (Fig. 2A–F). IgG deposits at DEJ, however, were similar in all of the strains (Fig. 2G–J). Consistent with these observations, we observed a high variation of skin blistering after anti-COL7 (vWFA2) IgG injection into genetically diverse advanced intercross line mice (Fig. 2K–O). Variances in the clinical phenotype in the inbred mouse lines were not associated with an enhanced immune response toward rabbit IgG. Interestingly, anti-rabbit IgG production was detected in all of the strains, except C57BL/6J mice ( $n = 11$ ). Among DBA/1J, BALB/c, and MRL/MpJ ( $n = 4$ /strain), similar anti-rabbit IgG ODs were measured (Supplemental Table I).

#### *Radiosensitive cells are responsible for the variation in clinical disease presentation in the end-stage effector phase of EBA*

To determine whether these differences in susceptibility to develop blisters are controlled by radiosensitive (hematopoietic) or non-radiosensitive cells or both, bone marrow chimeric mice were generated. First, to identify potential MHC-matched donor/recipient pairs and to exclude a possible impact of the MHC haplotype on blister induction, anti-COL7 (vWFA2) IgG was injected into MHC-congenic mouse strains of the B6 genetic background. C57BL/6J (H2b) mice were used as a reference. All MHC-congenic strains developed an identical clinical disease (Fig. 3A, 3B). The MHC-independent blister induction in MHC-congenic B6 mice, the resistance to EBA induction in MRL/MpJ (H2k) mice, and the susceptibility in B6.k mice collectively indicated that genes outside this locus control the susceptibility to autoantibody-induced tissue injury. Furthermore, this finding identified a MHC-matched donor/recipient pair for the generation of chimeric mice. Engraftment of either MRL/MpJ or B6.k bone marrow reached ~70%. Regardless of the recipient genotype, the recipients of MRL/MpJ bone marrow cells were nearly completely protected from skin blistering after the transfer of anti-COL7 (vWFA2) IgG. Conversely, B6.k bone marrow cells transferred to either recipient genotype did lead to severe clinical EBA manifestation (Fig. 3C–E).

#### *C57BL/6J and MRL/MpJ neutrophils differ in their response after activation with IC*

Because Gr-1 myeloid cells are the primary effector cells in experimental EBA (35), we evaluated whether neutrophils from C57BL/6J and MRL/MpJ differ in their response after stimulation.

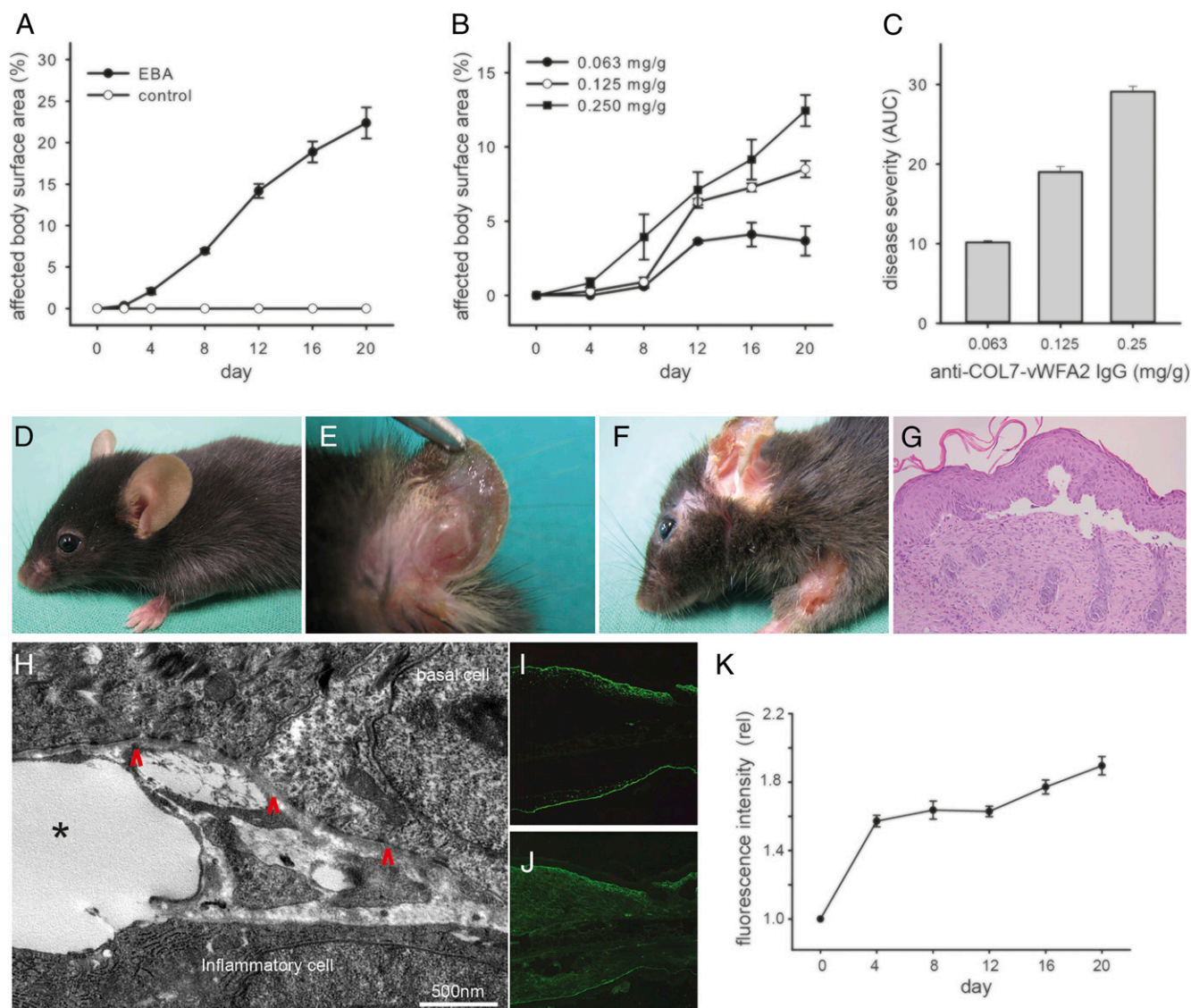


**FIGURE 1.** Transfer of anti-COL7vWFA2 IgG into C57BL/6 mice induces subepidermal blistering. **(A)** The mean  $\pm$  SEM of the body surface area (%) affected by skin lesions during the 20-d observation period in anti-COL7vWFA2 (EBA,  $n = 16$ ) or normal rabbit (control,  $n = 3$ ) IgG-injected C57BL/6 mice. **(B)** The induction of skin blistering by anti-COL7vWFA2 IgG into C57BL/6 mice is dose dependent ( $n = 3$ /group). **(C)** Cumulative disease severity, expressed as the area under the curve (AUC) and calculated from graph b. Clinical images of **(D)** normal rabbit or **(E and F)** anti-COL7vWFA2 IgG-injected C57BL/6 that were obtained at the end of the observation period. Whereas **(D)** normal rabbit IgG-injected mice showed no clinical disease, mice injected with immune IgG developed **(E)** blisters, **(F)** erosions, and crusts. **(G)** Histopathologically, subepidermal blistering and dense dermal inflammatory infiltrates were observed (original magnification  $\times 400$ ). **(H)** Using transmission electron microscopy, blister formation was observed below the lamina densa (arrowhead indicates the lamina densa; scale bar, 500 nm). Direct immunofluorescence microscopy showed **(I)** IgG and **(J)** C3 deposition at the DEJ. **(K)** The relative intensity of tissue-bound IgG at the DEJ increased during the observation period; comparison of the relative intensity of day 20 with all other time points showed a significant difference for all comparisons (one-way repeated measures ANOVA with Holm-Sidak posttest).

When stimulated with IC neutrophils derived from MRL/MpJ, bone marrow showed a significant reduced release of ROS compared with C57BL/6J mice (Fig. 4A, 4C). In contrast, when the cells were activated with PMA, no difference was observed between the two strains (Fig. 4B, 4C).

#### *Expression profiling of IC-activated neutrophils differs among EBA-susceptible and -resistant mouse strains*

To unravel the molecular basis for the different response to IC stimulation between MRL/MpJ and C57BL/6J mice, the cells were activated using IC, and global mRNA expression was compared between resting or activated neutrophils from MRL/MpJ or C57BL/6J mice. Unexpectedly, fewer genes ( $n = 44$ ) were differentially expressed in C57BL/6J after activation compared with

90 in MRL/MpJ mice (Fig. 5A). Of the differentially expressed genes, 35 were commonly differentially regulated in both strains, whereas 9 genes were only differentially regulated in C57BL/6J mice, in contrast to 55 in MRL/MpJ animals (Fig. 5). The complete expression data have been deposited at National Center for Biotechnology Information Gene Expression Omnibus (accession number GSE70193, <http://www.ncbi.nlm.nih.gov/geo/query/acc.cgi?acc=GSE70193>). These differentially expressed genes are predominantly allocated to four pathways in MRL/MpJ mice, more specifically, cytokine–cytokine receptor interaction (8 genes,  $p = 0.0001$ ), chemokine signaling (7 genes,  $p = 0.0001$ ), MAPK signaling (7 genes,  $p = 0.002$ ), as well as terpenoid backbone biosynthesis (2 genes,  $p = 0.002$ ). In C57BL/6J mice, only two pathways were found, that is, cytokine–cytokine receptor interaction



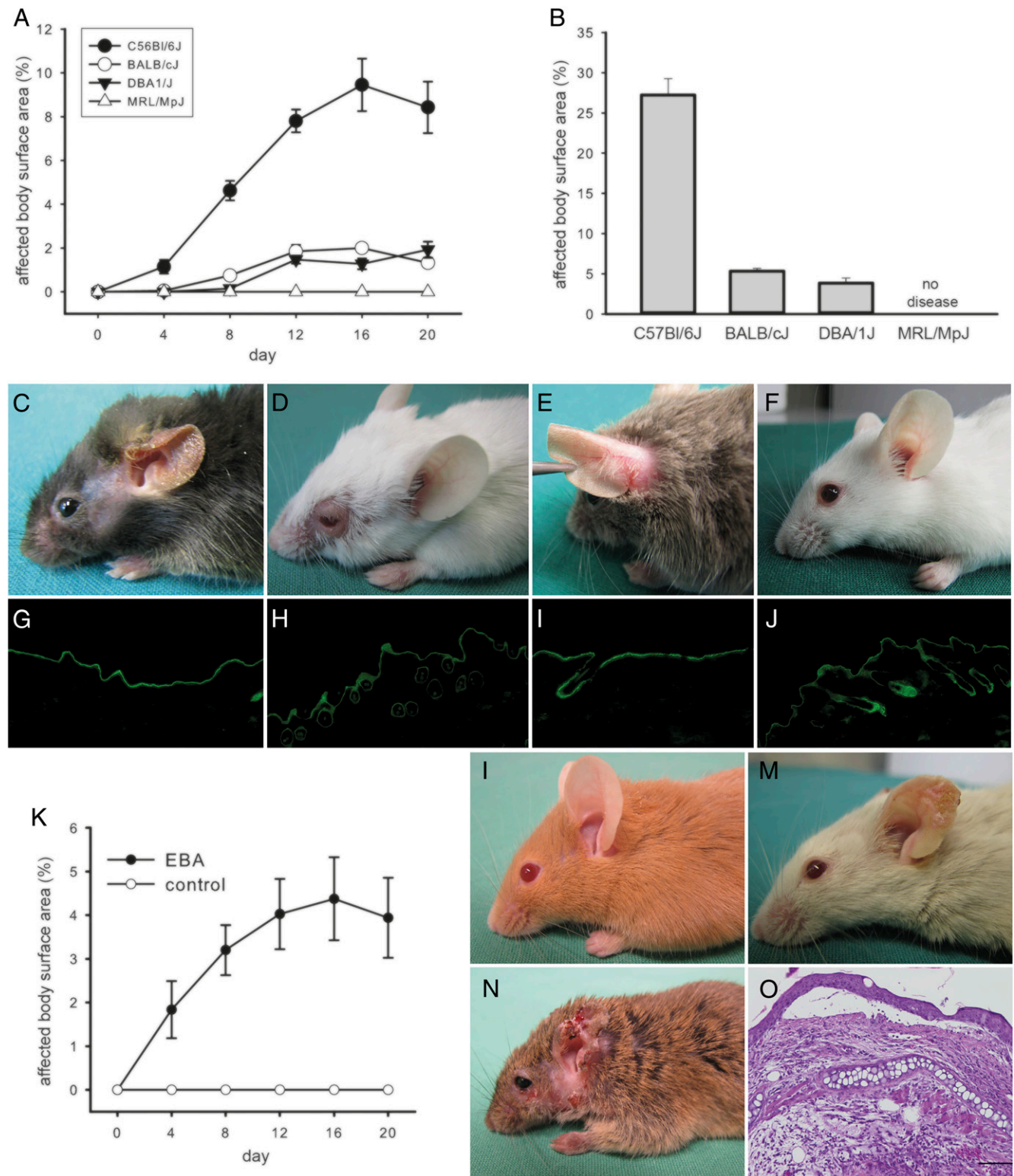


**FIGURE 2.** Induction of experimental EBA by autoantibody transfer in mice is strain dependent. **(A)** Disease score expressed as the percentage of the body surface area affected by skin lesions during the 20-d observation period in C57BL/6J, BALB/c, and MRL/MpJ mice ( $n = 4/\text{group}$ ) injected with immune IgG showed that C57BL/6J mice exhibited the most severe clinical phenotype, BALB/c mice had a mild phenotype, and MRL/MpJ mice showed no clinical signs. **(B)** The overall disease severity, scored as the area under the curve (calculated from the plots of affected body surface area against time from A), was significantly different between the four groups. **(C–F)** Representative clinical pictures of (C) a C57BL/6J mouse with a severe phenotype, (D) BALB/c and (E) DBA/1J mice with mild phenotypes, and (F) a MRL/MpJ mouse with no disease. **(G–J)** Direct IF revealed no differences in IgG deposits at the DEJ between the strains. **(K)** Advanced intercross line mice ( $n = 8$ ) developed clinical disease. **(L–N)** Representative clinical pictures of EBA-affected advanced intercross line mice. **(O)** H&E-stained skin section obtained from the lesional skin of an advanced intercross line mouse with evidence of subepidermal blistering and a dense, dermal leukocyte infiltration.

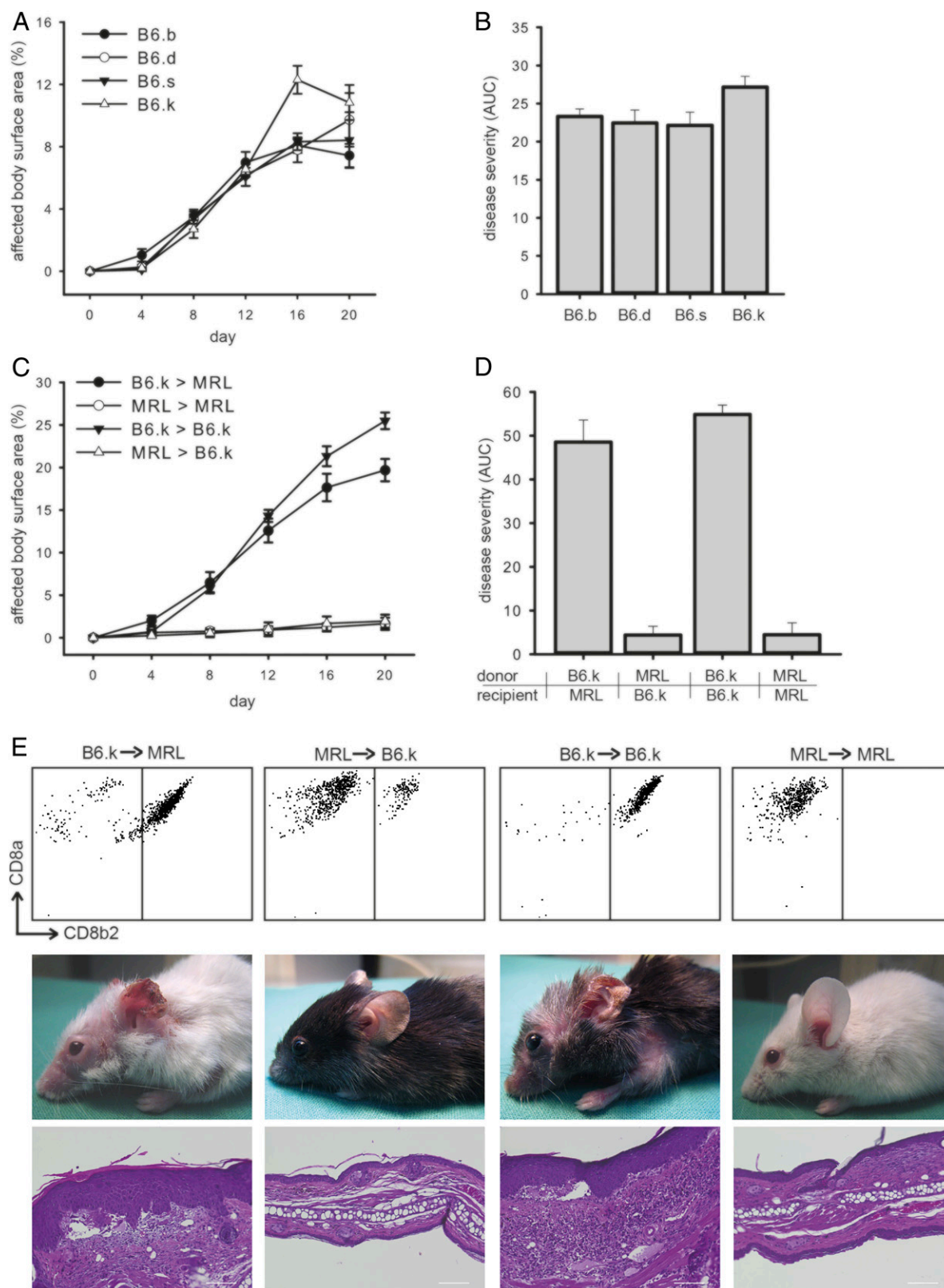
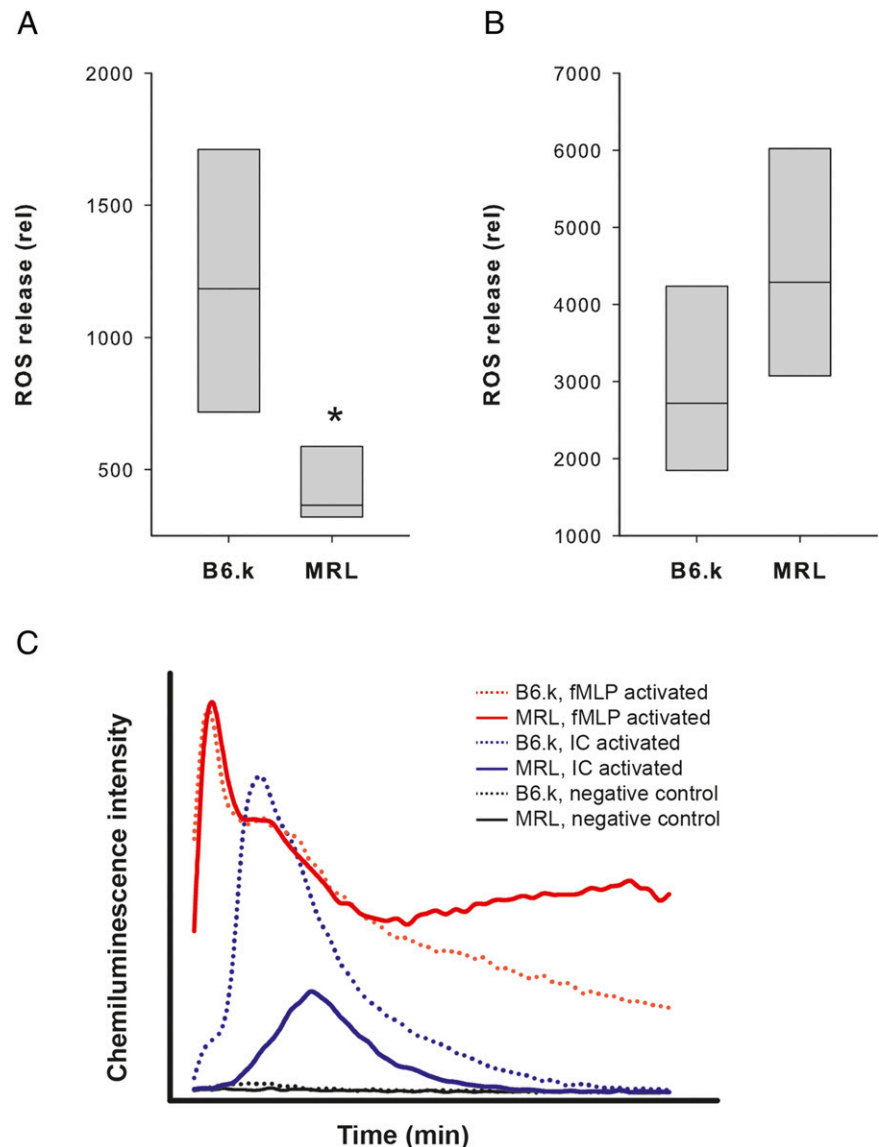


**FIGURE 3.** Radiosensitive cells are responsible for the varying clinical disease manifestations in the end-stage effector phase of EBA. **(A)** Disease scores, which were expressed as the percentage of the body surface area affected by skin lesions, in B6 mice carrying different MHC-H2 haplotypes (H2-b, -d, -s, and -k) showed similar disease severity in all groups ( $n = 6/\text{group}$ ). **(B)** Overall disease severity, scored as the area under the curve (AUC), was not significantly different between the groups. **(C)** Disease score over the duration of the experiment and **(D)** overall disease severity (AUC) in bone marrow chimeric mice. Independent of the donor strain, mice reconstituted with MRL/MpJ bone marrow were resistant to blister induction after anti-COL7 IgG transfer. In contrast, mice reconstituted with B6.k bone marrow developed severe clinical EBA. **(E)** Representative results from flow cytometry (upper panel), clinical images (middle panel), and H&E-stained sections from the ears of bone marrow chimeric mice (lower panel).

**FIGURE 4.** Distinct responses of neutrophils derived from C57BL/6J and MRL/MpJ mice are induced after stimulation with IC or PMA. Bone marrow–derived neutrophils from either C57BL/6J or MRL/MpJ mice were stimulated with (A) IC or (B) PMA, and their activation was assessed by measurement of ROS, which was normalized to resting cells of each strain ( $n = 4/\text{group}$ ). When stimulated with IC, the neutrophils from MRL mice showed a significantly lower degree of activation, whereas the stimulation using PMA showed no differences among the two strains. Due to the nonparametric distribution, data are presented as median (black line) and 75 percentiles (boxes).  $*p < 0.05$  (rank-sum test,  $n = 4$  mice/group). (C) Representative ROS release (chemiluminescence intensity) over time (0–60 min) in PMA (red)- or IC (blue)-stimulated neutrophils compared with resting cells (black) in MRL/MpJ (straight lines) and C57BL/6J mice (dotted lines).



(4 genes,  $p = 0.006$ ) and MAPK signaling (4 genes,  $p = 0.009$ ). This finding has been visualized by integrating the differential gene expression in the pathway analysis (Fig. 6).

## Discussion

Our data document a strain dependency in a novel Ab transfer-induced mouse model of EBA, a prototypical, organ-specific autoimmune disease. Using bone marrow chimeric mice, we were able to link this observation to radiosensitive cells. Our results from the different functional and transcriptional response of IC-activated neutrophils from EBA-resistant and EBA-susceptible mouse strains demonstrate that neutrophils of different inbred mouse lines have distinct responses to neutrophil agonists.

We had previously established a well-characterized Ab transfer-induced model reproducing the inflammatory variant of EBA (33). In an attempt to reproduce also the findings in the mechanobullous variant of EBA (14, 36), we immunized rabbits of the vWFA2 domain. This domain had been shown to be important for the interaction of COL7 with type I collagen (37), with the fibronectin 3-like domain 9 of COL7 (22) and the cysteine-knot located between the NC-1 and collagenous domain of COL7 (38). In this study, we show that Abs to the vWFA2 domain induce frank blistering when injected into wild-type mice. Interestingly,

however, blister formation in this model was also inflammation dependent, because, like in our previously described Ab transfer-induced EBA model (34), clinical disease manifestation was mediated by FcγR-induced inflammatory events. We were also intrigued by the distinct differences regarding the clinical phenotype in this novel Ab transfer-induced EBA model, which ranged from widespread blistering in C57BL/6J mice, in which up to 25% of the body surface area was affected by blistering and inflammatory skin lesions, to a complete absence of blistering in MRL/MpJ mice. Such strain differences have previously also been described in the K/B×N serum transfer arthritis mouse model (10) and in an immune-mediated nephritis model, induced by injection of anti-mouse glomerular basement membrane rabbit serum (11). In the latter model, the differences in nephritis were not due to an increased immune response to rabbit IgG, which we also observed in this study. Interestingly, in all three model systems, MRL/MpJ mice showed the least susceptibility to disease induction.

Intrigued by the striking differences in clinically evident blistering disease in the different inbred mouse lines, we aimed at excluding an impact of the MHC locus on Ab-induced blistering because this locus is a major susceptibility locus in immunization-induced EBA (9). The similar extent of blistering in MHC congenic B6 mice (H2d, H2k, H2s, and H2b as a control) in Ab



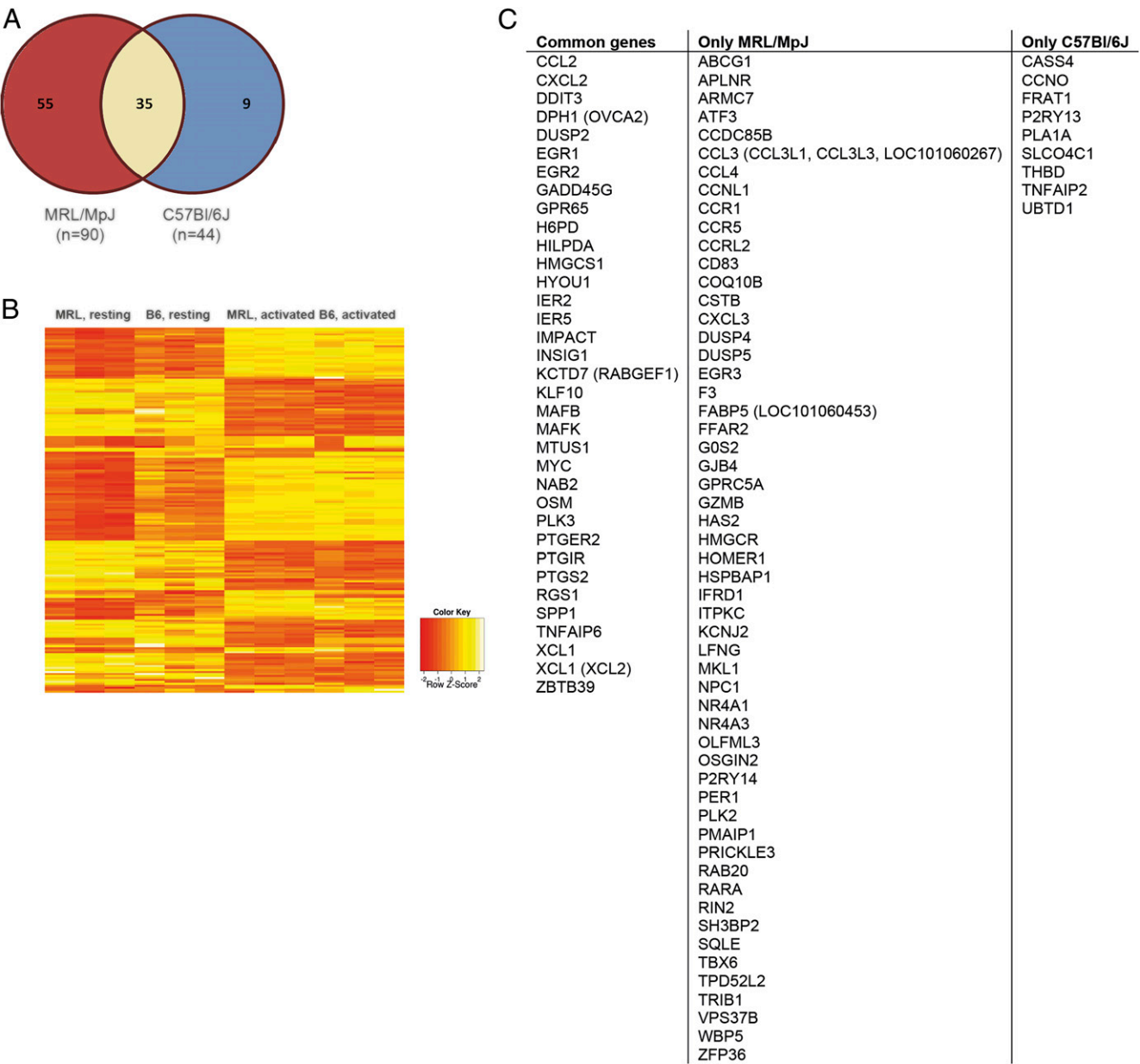


**FIGURE 5.** Distinct mRNA expression profile of IC-activated neutrophils from C57BL/6J and MRL/MpJ mice. **(A)** Venn diagram of differentially activated genes in IC-activated versus resting neutrophils in C57BL/6J and MRL/MpJ mice ( $n = 3$  mice per group and experimental condition). **(B)** Heat map of the differential expressed genes in the indicated mouse strains. **(C)** List of differentially expressed genes in MRL/MpJ and C57BL/6J mice after activation with IC. The data have been deposited at National Center for Biotechnology Information Gene Expression Omnibus (accession number GSE70193, <http://www.ncbi.nlm.nih.gov/geo/query/acc.cgi?acc=GSE70193>).

transfer-induced EBA, however, argues against a major contribution of the MHC locus in controlling the blistering phenotype. Additionally, these data identified a suitable donor/recipient pair to investigate the contribution of radiosensitive and nonradiosensitive cells to the observation of a strain dependency in autoantibody transfer-induced blistering in, more specifically, EBA-resistant MRK/MpJ (H2k) and EBA-susceptible B6.AK-H2k/FlaEgJ (B6.k) mice. We assumed that both cell types contribute to blistering because radiosensitive cells [i.e., Gr-1<sup>+</sup> myeloid cells (35)] and non-radiosensitive cells [i.e., complement proteins produced resident tissue cells and hepatocytes (33, 39)] have been shown to be required for blister induction. Interestingly, when hematopoietic cells from EBA-susceptible mice were used to rescue irradiated recipient mice, blistering was induced independent of the donor genotype. Conversely, when the cells from EBA-resistant mice were trans-

planted, none of the recipient mice developed blistering. Collectively, this finding indicates that radiosensitive, hematopoietic cells solely determine the strain dependency observed in this work. This is in contrast to observations noted in the K/B×N arthritis model, in which C5, which is predominantly produced in the liver, was identified as a major susceptibility locus (10).

Because ROS production by neutrophils is a key prerequisite for blister formation in experimental EBA (35), we compared the response to stimulation with IC of neutrophils from EBA-susceptible C57BL/6 to EBA-resistant MRL/MpJ mice. The results showed that the production of ROS after IC, but not after PMA, stimulation is significantly reduced in the EBA-resistant MRL/MpJ mice. This difference in the neutrophil response to stimulation with IC may, in part, explain the resistance of MRL/MpJ mice to the induction of experimental EBA by autoantibody transfer. This difference is also

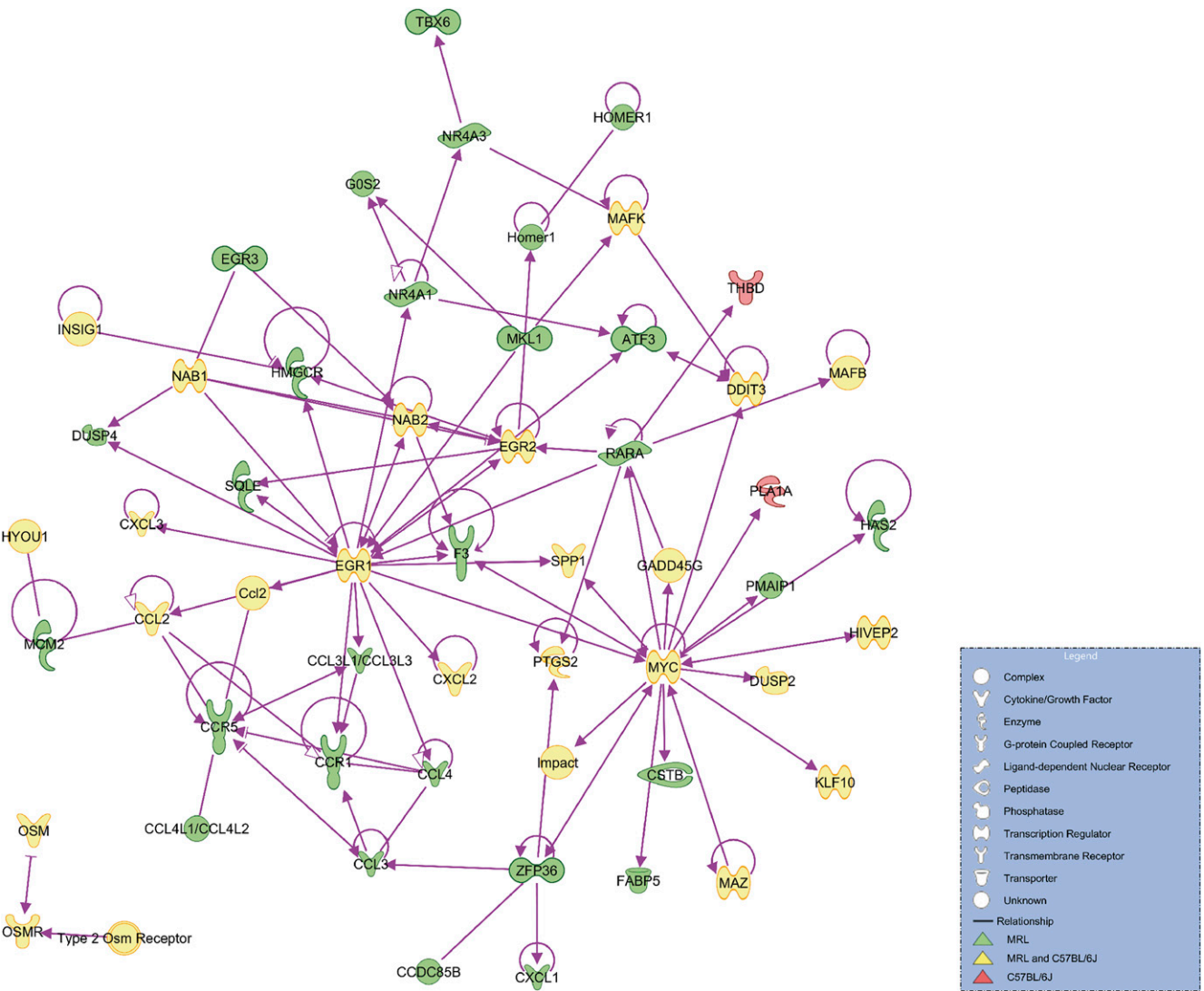


**FIGURE 6.** Network of differentially expressed genes of IC-activated neutrophils. The data shown in Fig. 5B were used for pathway analysis. This diagram illustrates the network by which the greater number of differential expressed genes in MRL/MpJ mice may modulate IC-induced activation.

reflected by the differential transcriptome response of neutrophils from these two strains after stimulation with IC. Based on the observed difference regarding IC-induced ROS release, we expected that more genes are differentially regulated in the EBA-susceptible C57BL/6J mice. Contrary to our assumptions, we found more differentially regulated genes in EBA-resistant MRL/MpJ mice. This may point toward the fact that, after IC binding, both inhibitory and activating signals are induced, that is, inhibitory signaling through the FcγRIIB or through dectin-1 (40). Therefore, it is tempting to speculate that the chemokine signaling and terpenoid backbone biosynthesis pathways can dampen the proinflammatory pathways, which is reflected by the cytokine–cytokine receptor interaction and MAPK signaling pathways.

These insights into the pathogenesis of experimental EBA and the transcriptome of IC-activated neutrophils from mice with a diverse response to neutrophil activation may aid the development of neutrophil-modulating strategies, which could provide therapeutic benefits in EBA, as well as in other neutrophil-dependent diseases.

### Acknowledgments

We thank Claudia Kauderer for providing excellent technical assistance.

### Disclosures

The authors have no financial conflicts of interest.

### References

1. Bach, J. F. 2002. The effect of infections on susceptibility to autoimmune and allergic diseases. *N. Engl. J. Med.* 347: 911–920.
2. Rose, N. R., and C. Bona. 1993. Defining criteria for autoimmune diseases (Witebsky's postulates revisited). *Immunol. Today* 14: 426–430.
3. Beutner, E. H., and R. E. Jordon. 1964. Demonstration of skin antibodies in sera of pemphigus vulgaris patients by indirect immunofluorescent staining. *Proc. Soc. Exp. Biol. Med.* 117: 505–510.
4. Rock, B., C. R. Martins, A. N. Theofilopoulos, R. S. Balderas, G. J. Anhalt, R. S. Labib, S. Futamura, E. A. Rivitti, and L. A. Diaz. 1989. The pathogenic effect of IgG4 autoantibodies in endemic pemphigus foliaceus (fogo selvagem). *N. Engl. J. Med.* 320: 1463–1469.
5. Reichert, J. M. 2012. Marketed therapeutic antibodies compendium. *MAbs* 4: 413–415.
6. Ludwig, R. J., K. Kalies, J. Köhl, D. Zillikens, and E. Schmidt. 2013. Emerging treatments for pemphigoid diseases. *Trends Mol. Med.* 19: 501–512.
7. Leontyev, D., Y. Katsman, and D. R. Branch. 2012. Mouse background and IVIG dosage are critical in establishing the role of inhibitory Fcγ receptor for the amelioration of experimental ITP. *Blood* 119: 5261–5264.
8. Watson, W. C., and A. S. Townes. 1985. Genetic susceptibility to murine collagen II autoimmune arthritis: proposed relationship to the IgG2 autoantibody subclass response, complement C5, major histocompatibility complex (MHC) and non-MHC loci. *J. Exp. Med.* 162: 1878–1891.
9. Ludwig, R. J., A. Recke, K. Bieber, S. Müller, Ade. C. Marques, D. Banczyk, M. Hirose, M. Kasperkiewicz, N. Ishii, E. Schmidt, et al. 2011. Generation of

- antibodies of distinct subclasses and specificity is linked to H2s in an active mouse model of epidermolysis bullosa acquisita. *J. Invest. Dermatol.* 131: 167–176.
10. Ji, H., D. Gauguier, K. Ohmura, A. Gonzalez, V. Duchatelle, P. Danoy, H. J. Garchon, C. Degott, M. Lathrop, C. Benoist, and D. Mathis. 2001. Genetic influences on the end-stage effector phase of arthritis. *J. Exp. Med.* 194: 321–330.
  11. Xie, C., R. Sharma, H. Wang, X. J. Zhou, and C. Mohan. 2004. Strain distribution pattern of susceptibility to immune-mediated nephritis. *J. Immunol.* 172: 5047–5055.
  12. Woodley, D. T., R. E. Burgeson, G. Lunstrum, L. Bruckner-Tuderman, M. J. Reese, and R. A. Briggaman. 1988. Epidermolysis bullosa acquisita antigen is the globular carboxyl terminus of type VII procollagen. *J. Clin. Invest.* 81: 683–687.
  13. Iwata, H., K. Bieber, B. Tiburzy, N. Chrobok, K. Kalies, A. Shimizu, S. Leineweber, A. Ishiko, A. Vorobyev, D. Zillikens, et al. 2013. B cells, dendritic cells, and macrophages are required to induce an autoreactive CD4 helper T cell response in experimental epidermolysis bullosa acquisita. *J. Immunol.* 191: 2978–2988.
  14. Buijsrogge, J. J., G. F. Diercks, H. H. Pas, and M. F. Jonkman. 2011. The many faces of epidermolysis bullosa acquisita after serration pattern analysis by direct immunofluorescence microscopy. *Br. J. Dermatol.* 165: 92–98.
  15. Zumelzu, C., C. Le Roux-Villet, P. Loiseau, M. Busson, M. Heller, F. Aucouturier, V. Pendaries, N. Lièvre, F. Pascal, M. D. Brette, et al. 2011. Black patients of African descent and HLA-DRB1\*15:03 frequency overrepresented in epidermolysis bullosa acquisita. *J. Invest. Dermatol.* 131: 2386–2393.
  16. Kim, J. H., Y. H. Kim, and S. C. Kim. 2011. Epidermolysis bullosa acquisita: a retrospective clinical analysis of 30 cases. *Acta Derm. Venereol.* 91: 307–312.
  17. Schmidt, E., and D. Zillikens. 2013. Pemphigoid diseases. *Lancet* 381: 320–332.
  18. Srinivas, G., S. Möller, J. Wang, S. Künzel, D. Zillikens, J. F. Baines, and S. M. Ibrahim. 2013. Genome-wide mapping of gene-microbiota interactions in susceptibility to autoimmune skin blistering. *Nat. Commun.* 4: 2462.
  19. Ledbetter, J. A., and L. A. Herzenberg. 1979. Xenogeneic monoclonal antibodies to mouse lymphoid differentiation antigens. *Immunol. Rev.* 47: 63–90.
  20. Ledbetter, J. A., R. V. Rouse, H. S. Micklem, and L. A. Herzenberg. 1980. T cell subsets defined by expression of Lyt-1,2,3 and Thy-1 antigens: two-parameter immunofluorescence and cytotoxicity analysis with monoclonal antibodies modifies current views. *J. Exp. Med.* 152: 280–295.
  21. Vorobyev, A., H. Ujiie, A. Recke, J. J. Buijsrogge, M. F. Jonkman, H. H. Pas, H. Iwata, T. Hashimoto, S. C. Kim, J. Hoon Kim, et al. 2015. Autoantibodies to multiple epitopes on the non-collagenous-1 domain of type VII collagen induce blisters. *J. Invest. Dermatol.* 135: 1565–1573.
  22. Leineweber, S., S. Schöning, and K. Seeger. 2011. Insight into interactions of the von-Willebrand-factor-A-like domain 2 with the FNIII-like domain 9 of collagen VII by NMR and SPR. *FEBS Lett.* 585: 1748–1752.
  23. Sadeghi, H., A. Lockmann, A. C. Hund, U. K. Samavedam, E. Pipi, K. Vafia, E. Hauenschild, K. Kalies, H. H. Pas, M. F. Jonkman, et al. 2015. Caspase-1-independent IL-1 release mediates blister formation in autoantibody-induced tissue injury through modulation of endothelial adhesion molecules. *J. Immunol.* 194: 3656–3663.
  24. Kasprick, A., X. Yu, J. Scholten, K. Hartmann, H. H. Pas, D. Zillikens, R. J. Ludwig, and F. Petersen. 2015. Conditional depletion of mast cells has no impact on the severity of experimental epidermolysis bullosa acquisita. *Eur. J. Immunol.* 45: 1462–1470.
  25. Iwata, H., E. Pipi, N. Möckel, P. Sondermann, A. Vorobyev, N. van Beek, D. Zillikens, and R. J. Ludwig. 2015. Recombinant soluble CD32 suppresses disease progression in experimental epidermolysis bullosa acquisita. *J. Invest. Dermatol.* 135: 916–919.
  26. Hirose, M., B. Tiburzy, N. Ishii, E. Pipi, S. Wende, E. Rentz, F. Nimmerjahn, D. Zillikens, R. A. Manz, R. J. Ludwig, and M. Kasperkiewicz. 2015. Effects of intravenous immunoglobulins on mice with experimental epidermolysis bullosa acquisita. *J. Invest. Dermatol.* 135: 768–775.
  27. Recke, A., L. M. Trog, H. H. Pas, A. Vorobyev, A. Abadpour, M. F. Jonkman, G. van Zandbergen, C. Kauderer, D. Zillikens, G. Vidarsson, and R. J. Ludwig. 2014. Recombinant human IgA1 and IgA2 autoantibodies to type VII collagen induce subepidermal blistering ex vivo. *J. Immunol.* 193: 1600–1608.
  28. Yu, X., K. Holdorf, B. Kasper, D. Zillikens, R. J. Ludwig, and F. Petersen. 2010. FcγRIIA and FcγRIIB are required for autoantibody-induced tissue damage in experimental human models of bullous pemphigoid. *J. Invest. Dermatol.* 130: 2841–2844.
  29. Hirahashi, J., D. Mekala, J. Van Ziffle, L. Xiao, S. Saffaripour, D. D. Wagner, S. D. Shapiro, C. Lowell, and T. N. Mayadas. 2006. Mac-1 signaling via Src-family and Syk kinases results in elastase-dependent thrombohemorrhagic vasculopathy. *Immunity* 25: 271–283.
  30. Hirose, M., A. Recke, T. Beckmann, A. Shimizu, A. Ishiko, K. Bieber, J. Westermann, D. Zillikens, E. Schmidt, and R. J. Ludwig. 2011. Repetitive immunization breaks tolerance to type XVII collagen and leads to bullous pemphigoid in mice. *J. Immunol.* 187: 1176–1183.
  31. Zillikens, D., K. Herzele, M. Georgi, E. Schmidt, I. Chimanovitch, H. Schumann, J. M. J. Mascaro, Jr., L. A. Diaz, L. Bruckner-Tuderman, E. B. Bröcker, and G. J. Giudice. 1999. Autoantibodies in a subgroup of patients with linear IgA disease react with the NC16A domain of BP180. *J. Invest. Dermatol.* 113: 947–953.
  32. Zillikens, D., Y. Kawahara, A. Ishiko, H. Shimizu, J. Mayer, C. V. Rank, Z. Liu, G. J. Giudice, H. H. Tran, M. P. Marinkovich, et al. 1996. A novel subepidermal blistering disease with autoantibodies to a 200-kDa antigen of the basement membrane zone. *J. Invest. Dermatol.* 106: 1333–1338.
  33. Sitaru, C., S. Mihai, C. Otto, M. T. Chiriac, I. Hausser, B. Dotterweich, H. Saito, C. Rose, A. Ishiko, and D. Zillikens. 2005. Induction of dermal-epidermal separation in mice by passive transfer of antibodies specific to type VII collagen. *J. Clin. Invest.* 115: 870–878.
  34. Kasperkiewicz, M., F. Nimmerjahn, S. Wende, M. Hirose, H. Iwata, M. F. Jonkman, U. Samavedam, Y. Gupta, S. Möller, E. Rentz, et al. 2012. Genetic identification and functional validation of FcγRIV as key molecule in autoantibody-induced tissue injury. *J. Pathol.* 228: 8–19.
  35. Chiriac, M. T., J. Roesler, A. Sindrilaru, K. Scharffetter-Kochanek, D. Zillikens, and C. Sitaru. 2007. NADPH oxidase is required for neutrophil-dependent autoantibody-induced tissue damage. *J. Pathol.* 212: 56–65.
  36. Roenigk, H. H. J., Jr., J. G. Ryan, and W. F. Bergfeld. 1971. Epidermolysis bullosa acquisita: report of three cases and review of all published cases. *Arch. Dermatol.* 103: 1–10.
  37. Wegener, H., S. Leineweber, and K. Seeger. 2013. The vWFA2 domain of type VII collagen is responsible for collagen binding. *Biochem. Biophys. Res. Commun.* 430: 449–453.
  38. Wegener, H., H. Paulsen, and K. Seeger. 2014. The cysteine-rich region of type VII collagen is a cystine knot with a new topology. *J. Biol. Chem.* 289: 4861–4869.
  39. Mihai, S., M. T. Chiriac, K. Takahashi, J. M. Thurman, V. M. Holers, D. Zillikens, M. Botto, and C. Sitaru. 2007. The alternative pathway of complement activation is critical for blister induction in experimental epidermolysis bullosa acquisita. *J. Immunol.* 178: 6514–6521.
  40. Karsten, C. M., M. K. Pandey, J. Figge, R. Kildenstein, P. R. Taylor, M. Rosas, J. U. McDonald, S. J. Orr, M. Berger, D. Petzold, et al. 2012. Anti-inflammatory activity of IgG1 mediated by Fc galactosylation and association of FcγRIIB and dextran-1. *Nat. Med.* 18: 1401–1406.